THE JOURNAL OF PHYSICAL CHEMISTRY Letters

Letter

pubs.acs.org/JPCL

Photonic Effects for Magnetic Dipole Transitions

Zijun Wang, Tim Senden, and Andries Meijerink*

Condensed Matter and Interfaces, Debye Institute for Nanomaterials Science, Utrecht University, Princetonplein 1, 3584 CC Utrecht, Netherlands

Supporting Information

ABSTRACT: The radiative transition probability is a fundamental property for optical transitions. Extensive research, theoretical and experimental, has been conducted to establish the relation between the photonic environment and electric dipole (ED) transition probabilities. Recent work shows that the nanocrystal (NC)-cavity model accurately describes the influence of the refractive index n on ED transition rates for emitters in NCs. For magnetic dipole (MD) transitions, theory predicts a simple n^3 dependence. However, experimental evidence is sparse and difficult to obtain. Here we report Eu^{3+}-(with distinct ED+MD transitions) and Gd^{3+}-(MD transitions) doped β-$NaYF_4$ NC model systems to probe the influence of n on ED and MD transition probabilities through luminescence lifetime and ED/MD intensity ratio measurements. The results provide strong experimental evidence for an n^3 dependence of MD transition probabilities. This insight is important for understanding and controlling the variation of spectral distribution in emission spectra by photonic effects.

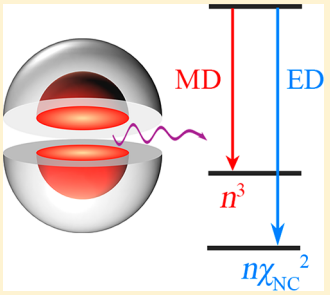

The spontaneous emission rate of an emitter is governed by Fermi's golden rule. Both transition dipole moments and photon density of states resonant with transitions affect the emission rate. The transition dipole moment depends on wave functions of initial and final states. For electric dipole (ED) transitions, the electromagnetic field strength interacting with the transition is influenced by the local environment and a local field correction factor χ is required. The transition probability k_{ED} is given by

$$k_{ED} = k_{ED}^0 n \chi^2 \tag{1}$$

where k_{ED} is the radiative decay rate of ED transition for the emitter in a dielectric medium with the refractive index n and k_{ED}^0 is the decay rate in vacuum ($n = 1$). The transition rate k is proportional to the local density of states (LDOS) and can be modified by tuning the dielectric medium surrounding the emitter.[1] The distance over which dielectric properties affect transition rates is of the order of the wavelength of the light emitted (hundreds of nanometers).[2] Extensive theoretical work has resulted in a variety of models for χ. The most prominent are the virtual[3−5] and real cavity[6−9] models which predict

$$k_{ED} = k_{ED}^0 n \left(\frac{n^2 + 2}{3}\right)^2 \tag{2}$$

$$k_{ED} = k_{ED}^0 n \left(\frac{3n^2}{2n^2 + 1}\right)^2 \tag{3}$$

For emitters doped in a nanocrystal (NC), the refractive index of the NC (n_{NC}) must be taken into consideration, giving rise to the NC-cavity model:[10]

$$k_{ED} = k_{ED}^0 n \left(\frac{3n^2}{2n^2 + n_{NC}^2}\right)^2 \tag{4}$$

The validity of the NC-cavity model was recently demonstrated by our group.[11,12]

In contrast to extensive research on photonic effects on ED transition rates, research on the influence of the local surroundings on magnetic dipole (MD) transitions is very limited. No local field effects are expected since the magnetic susceptibility (in a nonmagnetic medium) is the same as for vacuum, and thus a simple cubic dependence (reflecting the variation of photon density of states with n) is predicted:[13]

$$k_{MD} = k_{MD}^0 n^3 \tag{5}$$

where k_{MD} and k_{MD}^0 are the radiative decay rates of the MD transition for the emitter in a dielectric medium with refractive index n and in vacuum, respectively. Experimental results on the variation of MD transition rate with n are sparse as pure MD transitions are not often observed. In 1995, Rikken,[14] and later in 2002, Werts[15] reported on the influence of n on MD transition probabilities. Rikken studied Eu^{3+} complexes with distinct MD ($^5D_0$−$^7F_1$) and ED ($^5D_0$−$^7F_2$ and $^5D_0$−$^7F_4$) transitions. For the complexes dissolved in solvents with different n, the influence of n on the MD transition rates was measured and explained using the n^3 dependence. A good agreement was obtained taking into account partial quenching and a k_{MD}^0 of 10 s^{-1} for the $^5D_0$−$^7F_1$ transition. This rate is, however, significantly lower than the theoretically calculated k_{MD}^0 of 14.4 s^{-1}.[16] In the work by Werts, radiative lifetimes of

Received: September 27, 2017
Accepted: November 6, 2017
Published: November 7, 2017

DOI: 10.1021/acs.jpclett.7b02558
J. Phys. Chem. Lett. 2017, 8, 5689−5694

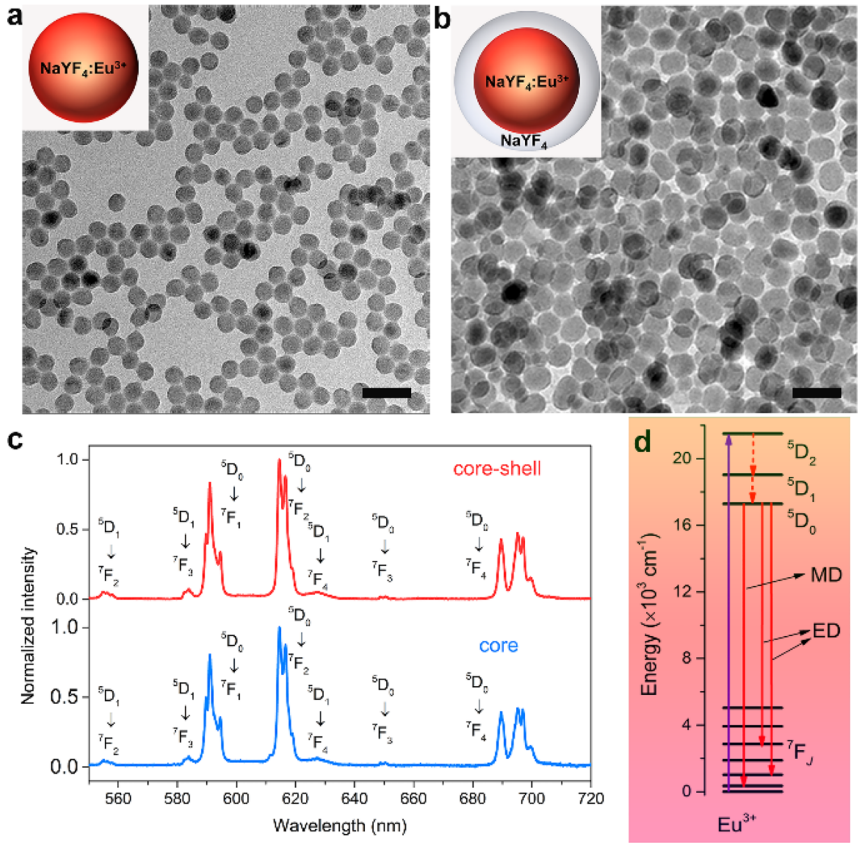

Figure 1. TEM images of (a) $NaY_{0.9}Eu_{0.1}F_4$ core and (b) $NaY_{0.9}Eu_{0.1}F_4$@$NaYF_4$ core−shell NCs (scale bar = 50 nm). (c) Emission spectra of core and core−shell NCs dispersed in chlorobenzene for 465 nm $^7F_0$−$^5D_2$ excitation. (d) Energy level diagram of Eu^{3+}. Emission in the orange/red spectral region includes forced ED ($^5D_0$−$^7F_2$, $^5D_0$−$^7F_4$) and MD ($^5D_0$−$^7F_1$) transitions.

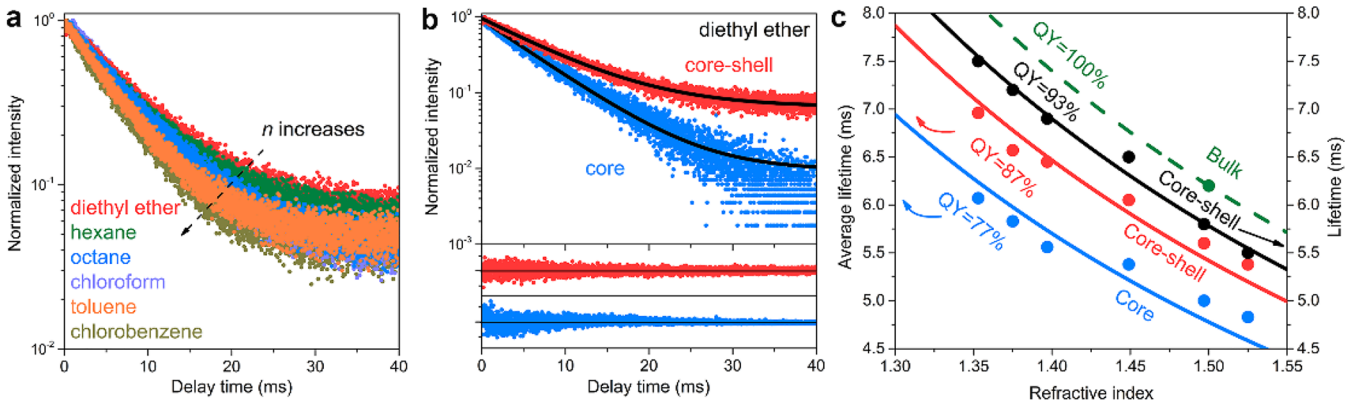

Figure 2. Decay curves of Eu^{3+} emission at 615 nm after pulsed 465 nm excitation for (a) $NaY_{0.9}Eu_{0.1}F_4$@$NaYF_4$ NCs in solvents with different n and for (b) core and core−shell NCs in diethyl ether with single exponential fits. Fit residuals are shown below. (c) Average lifetimes for $NaY_{0.9}Eu_{0.1}F_4$ (blue) and $NaY_{0.9}Eu_{0.1}F_4$@$NaYF_4$ (red) NCs. The black dots give lifetimes determined from a single exponential tail (t > 1 ms) fit for core−shell NCs. The green dashed line marks the radiative lifetime based on the bulk radiative lifetime and solvent refractive index. Drawn lines are fits to eq 6.

$Eu^{3+}$$^5D_0$ emission in a variety of materials were compared and related to the $^5D_0$−$^7F_1$ MD over the total (ED+MD) emission intensity ratio. Within the experimental accuracy (largely determined by significant uncertainties in quantum yield QY), a good agreement was obtained assuming an n^3 dependence of MD transition rate. In spite of these two insightful studies, a systematic and accurate investigation using model systems to study the relation between k_{MD} and n is still lacking. As shown previously, doped NCs serve as ideal probes for photonic effects.[11,12,17−21] The size of NCs is well below the hundreds of nanometers over which photonic effects influence transitions for emitters inside NCs. The local coordination of emitters is fixed in the nanocrystalline host and is the same as in bulk material. Because the local coordination is unaffected by the solvent surrounding NCs, an ideal model system is realized in which only the variation in solvent refractive index influences radiative decay rates of emitters inside NCs. In the present work, we report two NC model systems ($NaYF_4$:Eu^{3+} and $NaYF_4$:Gd^{3+}) to accurately determine the dependence of MD transition rates on n. The photonic effects in the present study involve a homogeneous dielectric medium with a limited range of n (1.35 to 1.53). In the past decades, a much wider variation

DOI: 10.1021/acs.jpclett.7b02558
J. Phys. Chem. Lett. 2017, 8, 5689−5694

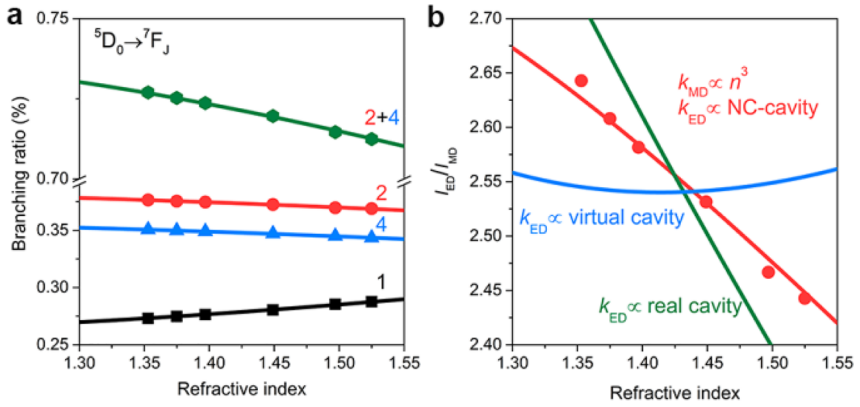

Figure 3. Variation of emission intensities for ED and MD transitions with n for $NaY_{0.9}Eu_{0.1}F_4$@$NaYF_4$ NCs. (a) Branching ratios of the MD $^5D_0-^7F_1$ (black), ED $^5D_0-^7F_2$ (red) and $^5D_0-^7F_4$ (blue) and total ED $^5D_0-^7F_2+^5D_0-^7F_4$ (green) transition intensities. Filled symbols show data and drawn lines are fits for an n^3 dependence for k_{MD} and a NC-cavity model dependence for k_{ED}. (b) Ratio of total ED and MD emission intensities (I_{ED}/I_{MD}). Colored lines are fits for an n^3 dependence of k_{MD} and the NC-cavity model (red line), virtual cavity (blue line) or real cavity (green line) model for the n dependence of k_{ED}.

in refractive index has been demonstrated in complex photonic and plasmonic structures, which give rise to much stronger variations in the luminescence properties.[22−26]

$NaYF_4$:Eu^{3+} and $NaYF_4$:Gd^{3+} NCs were synthesized using known colloidal synthesis techniques (see Supporting Information (SI) for details). Transmission electron microscope (TEM) images show monodisperse and nearly spherical ∼22 nm $NaY_{0.9}Eu_{0.1}F_4$ core NCs (Figure 1a) and slightly prolate ∼28 × 25 nm $NaY_{0.9}Eu_{0.1}F_4$@$NaYF_4$ core−shell NCs (Figure 1b). Oleate ligands on the surface allow the NCs to colloidally stabilize in apolar solvents with different n to investigate the influence of the photonic environment.[11,12] Six commonly used solvents are diethyl ether (n = 1.35), hexane (n = 1.38), octane (n = 1.40), chloroform (n = 1.45), toluene (n = 1.50), and chlorobenzene (n = 1.53). Figure 1c presents emission spectra for Eu^{3+}-doped core and core−shell NCs for $^5D_2$ excitation. Fast relaxation to the $^5D_0$ state is followed by radiative decay through both forced ED ($^5D_0-^7F_2$ at ∼615 nm and $^5D_0-^7F_4$ at ∼695 nm) and MD ($^5D_0-^7F_1$ at ∼590 nm) transitions. Variation of solvents does not affect the energy level structure resulting in identical emission spectra except for slight changes in relative intensities due to photonic effects (*vide infra*).

To investigate the relation between k_{MD} and n, we first consider the total $^5D_0$ decay rate. Figure 2a shows the decay curves of $^5D_0$ emission for core−shell NCs in different solvents (see also Figure S1). Ideally, the decay curves are single-exponential, but as a result of quenching, e.g., through coupling with high energy ligand vibrations, there is a contribution from nonradiative multiphonon relaxation (MPR), especially for Eu^{3+} ions close to the surface. The highest energy vibrational modes contributing are C−H stretching vibrations (∼3000 cm^{-1}) from oleate ligands on the NC surface and solvent molecules. For core−shell NCs, MPR is reduced. It affects only the initial decay and is similar for the different solvents. Two fitting procedures were used, based on the average lifetime τ_{avg} (see SI for details) and single exponential fitting. For core NCs, τ_{avg} of the $^5D_0$ state decreases from 6.1 to 4.8 ms upon increasing n from 1.35 to 1.53. A similar trend is observed for the core−shell NCs with longer luminescence lifetimes (7.0 ms vs 6.1 ms in core NCs in diethyl ether, Figure 2b) as the inert shell suppresses quenching by MPR.[27,28] Also, there is a stronger deviation from single exponential decay for Eu^{3+} in the core-only NCs. This deviation can be appreciated by comparing the fit residuals that show a systematic deviation for the initial part of the core-only decay curves.

The radiative rates k_r for individual $^5D_0-^7F_J$ transitions can be determined from the total radiative decay rate and relative emission intensities (branching ratio) derived from emission spectra. The nonradiative decay rate k_{nr} also contributes to the total decay rate and reduces QY. If the $^5D_0$ radiative lifetime for Eu^{3+} in bulk $NaYF_4$ is known, the upper limit of the QY of Eu^{3+}-doped NCs can be quantitatively determined using eq 6.

$$\tau_{avg} = QY\tau_{bulk}\Big/\left(\frac{I_{ED}}{I_{tot}}\frac{n\chi_{NC}^2}{n_{NC}} + \frac{I_{MD}}{I_{tot}}\frac{n^3}{n_{NC}^3}\right) \quad (6)$$

I_{ED}/I_{tot} and I_{MD}/I_{tot} denote the fractions of ED and MD emission in the total integrated emission intensity for $^5D_0-^7F_J$ transitions in bulk material. The NC-cavity local field factor χ_{NC} is used and τ_{bulk} is the $^5D_0$ lifetime of Eu^{3+} in bulk $NaYF_4$ (6.2 ms from measurements on bulk $NaY_{0.9}Eu_{0.1}F_4$, in excellent agreement with 6.2 ms reported by Tanner[29]). With τ_{bulk}, the observed branching ratios and n of $NaYF_4$ (1.5),[30] we find for k_{MD}^0 14.3 s^{-1} (very close to the theoretical value of 14.4 s^{-1})[16] and for k_{ED}^0 75.3 s^{-1}. To investigate the measured variation in radiative lifetime with n, Figure 2c plots τ_{avg} as a function of n. Fitting the data with eq 6 gives a good agreement using QYs of 77% and 87% for core and core−shell NCs, respectively. The slightly longer decay times derived from single exponential tail fits for core−shell NCs give an even higher QY of 93%. Note that actual QYs will be lower as the lifetimes reflect only emissive dopants in the ensemble.[12,31] Instead of QY, k_{nr} can be quantitatively determined to give a better agreement with experiment (Figure S2).

The analysis shows that the combination of an n^3 dependence for k_{MD} and the NC-cavity model for k_{ED} can quantitatively explain the observed variation of radiative decay rates. The good agreement between experiment and theory indicates that MD transition rates follow the theoretically predicted n^3 dependence. An alternative method to test the validity of the n^3 dependence is based on intensity ratios of ED and MD emission lines. Since nonradiative decay quenches both types of emission equally, the variation in ED/MD intensity ratio is a reliable method to test the n dependence of k_{MD} relative to k_{ED} without QY as additional fitting parameter. The difference in n dependence for k_{ED} and k_{MD} shows that

DOI: 10.1021/acs.jpclett.7b02558
J. Phys. Chem. Lett. 2017, 8, 5689−5694

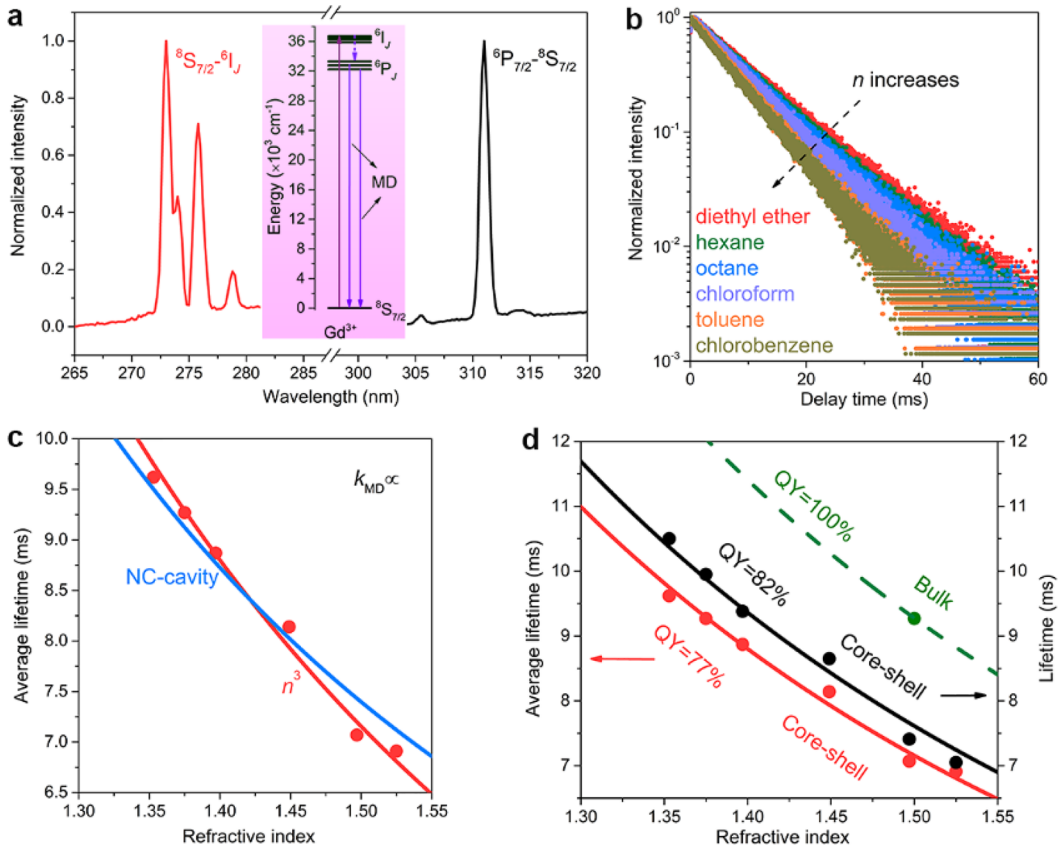

Figure 4. (a) Excitation (λ_{em} = 311 nm, red) and emission (λ_{ex} = 273 nm, black) spectra of $NaY_{0.95}Gd_{0.05}F_4$@$NaYF_4$ NCs in chlorobenzene. The inset shows the energy level diagram of Gd^{3+}. (b) Decay curves of 311 nm Gd^{3+} emission for core−shell NCs in solvents with different n. (c) Average lifetimes of the Gd^{3+} $^6P_{7/2}$−$^8S_{7/2}$ emission and fits for an n^3 k_{MD} dependence (red line) and the NC-cavity model (blue line). (d) Average Gd^{3+} emission lifetimes (red dots, same data as Figure 4c) and lifetimes from a single exponential tail (t > 1 ms) fit (black dots). The green broken line gives radiative lifetimes as a function of n based on the lifetime measured in bulk $NaYF_4$:Gd^{3+}. Drawn lines are fits to eq 7.

relative intensities of MD and ED transitions will change with n. The stronger n^3 dependence predicts an increase in relative intensity for MD emission lines with n. From the emission spectra the relative intensities of MD ($^5D_0$−$^7F_1$) and ED ($^5D_0$−$^7F_2$ and $^5D_0$−$^7F_4$) transitions were determined. Very weak emission lines corresponding to $^5D_0$−$^7F_{0,3,5,6}$ transitions are neglected in the present analysis. In Figure 3a, measured branching ratios for the MD and ED transitions are plotted together with the expected variation assuming an n^3 dependence for MD transitions (eq 5) and the NC-cavity model (eq 4) for ED transitions. The agreement is good and values for k^0_{MD} (14.4 s^{-1}) and k^0_{ED} (78.2 s^{-1}) are determined, which are consistent with theory and the results from bulk $NaYF_4$. To further verify the n dependence, Figure 3b shows the experimentally observed ratio I_{ED}/I_{MD} (red dots) and the red line shows the calculated ratio with k_{MD} proportional to n^3 with k^0_{MD} = 14.4 s^{-1} and k_{ED} following the NC-cavity model with k^0_{ED} (78.2 s^{-1}). Clearly, the n^3 dependence for k_{MD} is in excellent agreement with the experimentally observed ratios. The blue and green lines show fits for a fixed n^3 dependence for k_{MD} and different n dependencies for k_{ED}, viz., the virtual cavity model (eq 2, blue line) and the real cavity model (eq 3, green line). Only the NC-cavity model can explain the experimentally observed variation in I_{ED}/I_{MD} assuming an n^3 dependence for k_{MD}. The variation in I_{ED}/I_{MD} in the narrow refractive index range investigated here is limited (see Figure 3). However, intensity ratio changes over an order of magnitude can be realized by making use of high refractive index materials based on metal or semiconductor nanostructures.[32−34] This will allow a complete reversal of ED to MD intensities for emitters showing both types of emission.

To provide further evidence for the n^3 dependence of k_{MD}, we also investigated the decay times of MD emission from Gd^{3+}. Gd^{3+} has the $4f^7$ configuration and the first excited state ($^6P_{7/2}$) for this stable half-filled shell configuration is in the UV. The $^6P_{7/2}$−$^8S_{7/2}$ emission is around 311 nm and has a large MD transition probability (high value for the MD matrix element (L +2S) of −0.52).[35] Using this value, the MD transition rate for the $^6P_{7/2}$−$^8S_{7/2}$ transition in bulk $NaYF_4$ is k_{MD} = 102 s^{-1} (τ = 9.8 ms, see SI for details). This value is very close to the observed bulk decay rate (k = 108 s^{-1} for τ = 9.3 ms). This confirms that the $^6P_{7/2}$−$^8S_{7/2}$ transition of Gd^{3+} in $NaYF_4$ has 95% MD character,[36,37] which makes the Gd^{3+} $^6P_{7/2}$−$^8S_{7/2}$ emission ideal for investigating the influence of n on MD transition probabilities. The emission spectrum of Gd^{3+}-doped NCs is shown in Figure 4a. For the narrow $^6P_{7/2}$−$^8S_{7/2}$ emission around 311 nm the decay dynamics are shown in Figure 4b in solvents with different n (see also Figure S3). Upon increasing n from 1.35 to 1.53 the $^6P_{7/2}$ lifetime decreases from 9.6 to 6.9 ms (Figure 4c). The results are fitted to an n^3 dependence (eq 5). An excellent agreement is observed, confirming that the MD transition probability increases with n^3 as expected theoretically. Alternatively, this n^3 dependence of k_{MD} is confirmed by n^a fits in Figure S4. This n^3 dependence is stronger than the n dependence for ED transitions. As a result, the branching ratio in an emission spectrum consisting of mixed

DOI: 10.1021/acs.jpclett.7b02558
J. Phys. Chem. Lett. 2017, 8, 5689−5694

MD and ED transitions will change and the relative intensity of MD transitions will increase with n (see also Figure 3a). From the radiative lifetime of Gd^{3+} emission in bulk $NaYF_4$, we can calculate radiative lifetimes for emission in different solvents (*vide supra*). The calculated lifetimes are longer than the observed lifetimes, indicating that there is some quenching of the luminescence, probably by trace amounts of UV-absorbing organic chromophores in the solvents.[38,39] The QY of Gd^{3+} emission in core−shell NCs is determined by fitting the experimentally observed lifetimes to

$$\tau_{avg} = QY\tau_{bulk}n_{NC}^3/n^3 \quad (7)$$

In Figure 4d the results are shown. A good agreement between experiment and theory is obtained for a QY of 77% for τ_{avg} and 82% for the tail fitting results.

In conclusion, the influence of the photonic environment on MD transition probabilities has been systematically investigated using Eu^{3+}- and Gd^{3+}-doped $NaYF_4$ NCs as model systems. Varying the refractive index of the solvent in which NCs are dispersed reveals a strong increase of the MD transition probability with n. For Eu^{3+}-doped NCs, all experimental results (ED/MD intensity ratios and decay rates) are in excellent agreement with the theoretically predicted n^3 dependence for MD transition probabilities if the variation in ED transition probability is assumed to obey the NC-cavity model. For Gd^{3+}, the variation in MD transition probability can be directly assessed as the $^6P_{7/2}$−$^8S_{7/2}$ transition has 95% MD character. The strong refractive index dependence of the $^6P_{7/2}$ decay time closely follows the theoretical n^3 dependence providing further experimental evidence for the n^3 dependence of MD transition probabilities. The present study is the first systematic and accurate investigation providing convincing experimental evidence for the theoretically predicted n^3 dependence of MD transition probabilities. Insights in the influence of the local environment on radiative transitions are important for understanding and controlling optical properties through variations in the photonic environment.

■ ASSOCIATED CONTENT

Supporting Information

The Supporting Information is available free of charge on the ACS Publications website at DOI: 10.1021/acs.jpclett.7b02558.

Experimental methods, average lifetimes, luminescence decay curves, nonradiative decay rates, MD transition probability calculation, and fits for n^a dependence (PDF)

■ AUTHOR INFORMATION

Corresponding Author

*E-mail: A.Meijerink@uu.nl.

ORCID

Andries Meijerink: 0000-0003-3573-9289

Notes

The authors declare no competing financial interest.

■ ACKNOWLEDGMENTS

We thank F. T. Rabouw and P. T. Prins for the useful discussions. This work was financially supported by the China Scholarship Council (No. 201506380101).

■ REFERENCES

(1) Toptygin, D. Effects of the Solvent Refractive Index and Its Dispersion on the Radiative Decay Rate and Extinction Coefficient of a Fluorescent Solute. *J. Fluoresc.* **2003**, *13*, 201−219.

(2) Aubret, A.; Pillonnet, A.; Houel, J.; Dujardin, C.; Kulzer, F. CdSe/ZnS Quantum Dots as Sensors for the Local Refractive Index. *Nanoscale* **2016**, *8*, 2317−2325.

(3) de Vries, P.; Lagendijk, A. Resonant Scattering and Spontaneous Emission in Dielectrics: Microscopic Derivation of Local-Field Effects. *Phys. Rev. Lett.* **1998**, *81*, 1381−1384.

(4) Duan, C. K.; Reid, M. F. Local Field Effects on the Radiative Lifetimes of Ce^{3+} in Different Hosts. *Curr. Appl. Phys.* **2006**, *6*, 348−350.

(5) Duan, C. K.; Wen, H. L.; Tanner, P. A. Local-Field Effect on the Spontaneous Radiative Emission Rate. *Phys. Rev. B: Condens. Matter Mater. Phys.* **2011**, *83*, 245123.

(6) Glauber, R. J.; Lewenstein, M. Quantum Optics of Dielectric Media. *Phys. Rev. A: At., Mol., Opt. Phys.* **1991**, *43*, 467−491.

(7) Kumar, G. M.; Rao, D. N.; Agarwal, G. S. Measurement of Local Field Effects of the Host on the Lifetimes of Embedded Emitters. *Phys. Rev. Lett.* **2003**, *91*, 203903.

(8) Schuurmans, F. J. P.; de Lang, D. T. N.; Wegdam, G. H.; Sprik, R.; Lagendijk, A. Local-Field Effects on Spontaneous Emission in a Dense Supercritical Gas. *Phys. Rev. Lett.* **1998**, *80*, 5077−5080.

(9) Zhu, Y. S.; Xu, W.; Zhang, H. Z.; Wang, W.; Tong, L.; Xu, S.; Sun, Z. P.; Song, H. W. Highly Modified Spontaneous Emissions in YVO_4:Eu^{3+} Inverse Opal and Refractive Index Sensing Application. *Appl. Phys. Lett.* **2012**, *100*, 081104.

(10) Duan, C. K.; Reid, M. F. Macroscopic Models for the Radiative Relaxation Lifetime of Luminescent Centers Embedded in Surrounding Media. *Spectrosc. Lett.* **2007**, *40*, 237−246.

(11) Rabouw, F. T.; den Hartog, S. A.; Senden, T.; Meijerink, A. Photonic Effects on the Förster Resonance Energy Transfer Efficiency. *Nat. Commun.* **2014**, *5*, 3610.

(12) Senden, T.; Rabouw, F. T.; Meijerink, A. Photonic Effects on the Radiative Decay Rate and Luminescence Quantum Yield of Doped Nanocrystals. *ACS Nano* **2015**, *9*, 1801−1808.

(13) Nienhuis, G.; Alkemade, C. Th. J Atomic Radiative Transition Probabilities in a Continuous Medium. *Physica B+C* **1976**, *81*, 181−188.

(14) Rikken, G. L. J. A.; Kessener, Y. A. R. R. Local Field Effects and Electric and Magnetic Dipole Transitions in Dielectrics. *Phys. Rev. Lett.* **1995**, *74*, 880−883.

(15) Werts, M. H. V.; Jukes, R. T. F.; Verhoeven, J. W. The Emission Spectrum and the Radiative Lifetime of Eu^{3+} in Luminescent Lanthanide Complexes. *Phys. Chem. Chem. Phys.* **2002**, *4*, 1542−1548.

(16) Dodson, C. M.; Zia, R. Magnetic Dipole and Electric Quadrupole Transitions in the Trivalent Lanthanide Series: Calculated Emission Rates and Oscillator Strengths. *Phys. Rev. B: Condens. Matter Mater. Phys.* **2012**, *86*, 125102.

(17) Meltzer, R. S.; Feofilov, S. P.; Tissue, B.; Yuan, H. B. Dependence of Fluorescence Lifetimes of Y_2O_3:Eu^{3+} Nanoparticles on the Surrounding Medium. *Phys. Rev. B: Condens. Matter Mater. Phys.* **1999**, *60*, R14012−R14015.

(18) Wuister, S. F.; de Mello Donegá, C.; Meijerink, A. Local-Field Effects on the Spontaneous Emission Rate of CdTe and CdSe Quantum Dots in Dielectric Media. *J. Chem. Phys.* **2004**, *121*, 4310−4315.

(19) Aigouy, L.; Cazé, A.; Gredin, P.; Mortier, M.; Carminati, R. Mapping and Quantifying Electric and Magnetic Dipole Luminescence at the Nanoscale. *Phys. Rev. Lett.* **2014**, *113*, 076101.

(20) Rabouw, F. T.; Prins, P. T.; Norris, D. J. Europium-Doped $NaYF_4$ Nanocrystals as Probes for the Electric and Magnetic Local Density of Optical States throughout the Visible Spectral Range. *Nano Lett.* **2016**, *16*, 7254−7260.

(21) Pillonnet, A.; Fleury, P.; Chizhik, A. I.; Chizhik, A. M.; Amans, D.; Ledoux, G.; Kulzer, F.; Meixner, A. J.; Dujardin, C. Local Refractive Index Probed via the Fluorescence Decay of Semiconductor Quantum Dots. *Opt. Express* **2012**, *20*, 3200−3208.

DOI: 10.1021/acs.jpclett.7b02558
J. Phys. Chem. Lett. 2017, 8, 5689−5694

(22) Karaveli, S.; Zia, R. Spectral Tuning by Selective Enhancement of Electric and Magnetic Dipole Emission. *Phys. Rev. Lett.* **2011**, *106*, 193004.
(23) Choi, B.; Iwanaga, M.; Sugimoto, Y.; Sakoda, K.; Miyazaki, H. T. Selective Plasmonic Enhancement of Electric- and Magnetic-Dipole Radiations of Er Ions. *Nano Lett.* **2016**, *16*, 5191−5196.
(24) Noda, S.; Fujita, M.; Asano, T. Spontaneous-Emission Control by Photonic Crystals and Nanocavities. *Nat. Photonics* **2007**, *1*, 449−458.
(25) Leistikow, M. D.; Mosk, A. P.; Yeganegi, E.; Huisman, S. R.; Lagendijk, A.; Vos, W. L. Inhibited Spontaneous Emission of Quantum Dots Observed in a 3D Photonic Band Gap. *Phys. Rev. Lett.* **2011**, *107*, 193903.
(26) Curto, A. G.; Volpe, G.; Taminiau, T. H.; Kreuzer, M. P.; Quidant, R.; van Hulst, N. F. Unidirectional Emission of a Quantum Dot Coupled to a Nanoantenna. *Science* **2010**, *329*, 930−933.
(27) Wang, F.; Wang, J.; Liu, X. G. Direct Evidence of a Surface Quenching Effect on Size-Dependent Luminescence of Upconversion Nanoparticles. *Angew. Chem., Int. Ed.* **2010**, *49*, 7456−7460.
(28) Wang, Z. J.; Zhang, Y. L.; Zhong, J. P.; Yao, H. H.; Wang, J.; Wu, M. M.; Meijerink, A. One-Step Synthesis and Luminescence Properties of Tetragonal Double Tungstates Nanocrystals. *Nanoscale* **2016**, *8*, 15486−15489.
(29) Jia, G. H.; Tanner, P. A. Energy Transfer between UO_2^{2+} and Eu^{3+} in β-$NaYF_4$. *J. Alloys Compd.* **2009**, *471*, 557−560.
(30) Ivaturi, A.; MacDougall, S. K. W.; Martín-Rodríguez, R.; Quintanilla, M.; Marques-Hueso, J.; Krämer, K. W.; Meijerink, A.; Richards, B. S. Optimizing Infrared to Near Infrared Upconversion Quantum Yield of β-$NaYF_4$:Er^{3+} in Fluoropolymer Matrix for Photovoltaic Devices. *J. Appl. Phys.* **2013**, *114*, 013505.
(31) Würth, C.; Geißler, D.; Behnke, T.; Kaiser, M.; Resch-Genger, U. Critical Review of the Determination of Photoluminescence Quantum Yields of Luminescent Reporters. *Anal. Bioanal. Chem.* **2015**, *407*, 59−78.
(32) Shin, J.; Shen, J.-T.; Fan, S. H. Three-Dimensional Metamaterials with an Ultrahigh Effective Refractive Index over a Broad Bandwidth. *Phys. Rev. Lett.* **2009**, *102*, 093903.
(33) Savelev, R. S.; Makarov, S. V.; Krasnok, A. E.; Belov, P. A. From Optical Magnetic Resonance to Dielectric Nanophotonics. *Opt. Spectrosc.* **2015**, *119*, 551−568.
(34) Kuznetsov, A. I.; Miroshnichenko, A. E.; Brongersma, M. L.; Kivshar, Y. S.; Luk'yanchuk, B. Optically Resonant Rielectric Nanostructures. *Science* **2016**, *354*, aag2472.
(35) Detrio, J. A. Line Strengths for Gd^{3+} at a C_{4v} Site in SrF_2. *Phys. Rev. B: Solid State* **1971**, *4*, 1422−1427.
(36) Sytsma, J.; van Schaik, W.; Blasse, G. Vibronic Transitions in the Emission Spectra of Gd^{3+} in Several Rare-Earth Compounds. *J. Phys. Chem. Solids* **1991**, *52*, 419−429.
(37) Binnemans, K.; Görller-Walrand, C.; Adam, J. L. Spectroscopic Properties of Gd^{3+}-Doped Fluorozirconate Glass. *Chem. Phys. Lett.* **1997**, *280*, 333−338.
(38) Buono-Core, G. E.; Li, H.; Marciniak, B. Quenching of Excited States by Lanthanide Ions and Chelates in Solution. *Coord. Chem. Rev.* **1990**, *99*, 55−87.
(39) de Sá, G. F.; Malta, O. L.; de Mello Donegá, C.; Simas, A. M.; Longo, R. L.; Santa-Cruz, P. A.; da Silva, E. F., Jr. Spectroscopic Properties and Design of Highly Luminescent Lanthanide Coordination Complexes. *Coord. Chem. Rev.* **2000**, *196*, 165−195.

DOI: 10.1021/acs.jpclett.7b02558
J. Phys. Chem. Lett. 2017, 8, 5689−5694